Climate Risk Management 38 (2022) 100459

Contents lists available at ScienceDirect

Climate Risk Management

journal homepage: www.elsevier.com/locate/crm

Changes in global heat waves and its socioeconomic exposure in a warmer future

Cong Yin [a,b,c], Yaping Yang [a,c,d,*], Xiaona Chen [a,c], Xiafang Yue [a,c], Yangxiaoyue Liu [a,c], Ying Xin [a,b,c]

[a] State Key Laboratory of Resources and Environmental Information System, Institute of Geographic Sciences and Natural Resources Research, Chinese Academy of Sciences, Beijing 100101, China
[b] College of Resources and Environment, University of Chinese Academy of Sciences, Beijing 100049, China
[c] National Earth System Science Data Center, Beijing 100101, China
[d] Jiangsu Center for Collaborative Innovation in Geographical Information Resource Development and Application, Nanjing 210023, China

ARTICLE INFO

Keywords:
Heat wave
Exposure
Risk
SSPs
Spatiotemporal
Socioeconomic

ABSTRACT

Heat waves are continuous high temperature processes, which are defined as the daily maximum temperature exceeding the absolute-relative combined high temperature thresholds for more than three consecutive days in this study. Because of its unprecedented casualties, devastating compound disasters and irreversible deterioration trends, heat waves have attracted worldwide concern, while its global changes and socioeconomic impacts still need further study. Using three historical reanalysis data and multi scenario CMIP6 modeled data, Global Heat Wave Toolbox (GHWT) was developed to generate heat wave matrix from 1971 to 2100. The long-term changing characteristics of global heat waves were also analyzed. Next, population and GDP projections are employed to estimate future socioeconomic exposure and risks. The results show that except for high latitudes (latitude greater than 60°), high elevations and some coastal areas, heat waves have visited about 45% (±3%) of the global land area (excluding Antarctica). North Africa, North Australia, South Asia, and the Arabian Peninsula are detected as high heat wave area, where experience more than three heat waves with total duration over 15 days annually. Additionally, the average growth rate of global heat waves under SSP2 4.5 and SSP5 8.5 may be 2–3 times and 3–5 times of that under SSP1 2.6, respectively. Under SSP2 4.5, there may be about 7.32 billion people exposed to heat waves in 2100, accounting for 82.65% of the global population. Economic exposure may reach $433.37 trillion in 2100, accounting for 82.23% of the total global economy in that year. India could have the highest population and economic exposure, follow by populous countries, such as Pakistan and Bangladesh, and major economies, such as China and the United States. Under SSP1 2.6, the increase in heat waves may slow down significantly. Moreover, North Africa, Australia, and Brazil are identified as rapid heat wave growth area. Our study highlights the heat wave of future growth and its socioeconomic impacts, as well as the necessity for climate mitigation and adaptation measures.

* Corresponding author.
E-mail address: yangyp@igsnrr.ac.cn (Y. Yang).

https://doi.org/10.1016/j.crm.2022.100459
Received 14 May 2022; Received in revised form 15 September 2022; Accepted 15 September 2022
Available online 16 September 2022

1. Introduction

Heat wave, as a typical climate extreme, have been highly emphasized in the new released IPCC 6th Assessment Report. And it is reported that the frequency, duration and intensity of hot extremes and heat waves have increased since 1950 and will further increase in the future even if global warming is stabilized at 1.5 °C (Masson-Delmotte et al., 2021). Because of unprecedented casualties (Roye et al., 2020, Yang et al., 2019), devastating compound disasters (Parente et al., 2018, Schumacher et al., 2019) and irreversible deterioration trends (Meehl and Tebaldi, 2004, Perkins et al., 2012, Perkins-Kirkpatrick and Lewis, 2020), the worldwide heat waves have attracted widespread attention. In late June to middle July of 2021, heat waves in Western North America caused more than 900 deaths and wildfires covering hundreds of square kilometers (Johnson, 2021, Potestio, 2021). Accompanying with the historic Western Europe heat wave in the summer of 2003 (Stott et al., 2004, Mitchell et al., 2019), the catastrophic heat waves in developed regions have evidenced that even in the regions with advanced administrative and medical experience, heat waves can also lead to disastrous consequences. Moreover, the severe consequences caused by heat waves are not only derived from the severity of the events, but also the events are tending to visit novel regions, where the emergency infrastructure and experience is obviously deficient (Dubey et al., 2021, Wondmagegn et al., 2021). For example, British Columbia held the highest temperature record in the 2021 North America heat wave, and Western Canada has set 103 all-time high temperature records (Uguen-Csenge, 2021). As heat waves are drastically changing and bringing great losses, it is urgently needed to investigate their spatiotemporal variation pattern and long-term changing trend to practice disaster risk reduction measures. Additionally, climate risks are likely to be further exacerbated by humanity's relative lack of adaptation. Consequently, identifying regions with high heat wave exposure and risks in the future is also meaningful for residents and policy makers.

Recent studies have made great progress in using predictive and integrative perspectives to investigate heat waves and their socioeconomic impacts (Zittis et al., 2021, Tuholske et al., 2021, Garcia-Leon et al., 2021). More coupled indices, models and methods, such as WBGT (Wet-Bulb Globe Temperature), CESM (Community Earth System Model) and CGE (Computable General Equilibrium), are used to analyze the changes, drivers, and impacts of heat waves (Ullah et al., 2022, Tuholske et al., 2021, Garcia-Leon et al., 2021, Chen et al., 2020, Founda et al., 2020). These studies can be divided into macro and micro levels. The macro level studies aim to investigate the variation pattern of heat waves over large spatial scales or longtime series, like its frequency, duration, intensity, exposure, vulnerability, and risk, etc. (Sun et al., 2018, Wang et al., 2020, Yin et al., 2020, Dong et al., 2020, Yamagata et al., 2019). Yu et al. detected significant positive trends in the frequency and amplitude of wet heat waves in most areas of Eurasia during summer from 1979 to 2017 (Yu et al., 2021). Wang et al. highlighted a higher risks to human body caused by night heat wave (Wang et al., 2020). Yin et al. identified eastern China, northern South Asia, and some highly populated cities as high heat wave risk areas (Yin et al., 2020). The micro level studies pay close attention to the natural and socioeconomic effects induced by heat waves, such as human health damage (Amengual et al., 2014), labor productivity loss (Zhao et al., 2021, Liu et al., 2021), medical and economic burden rise (Wondmagegn et al., 2021, Borg et al., 2021), crop yields decline (van der Velde et al., 2010) and ecosystem productivity change (Bastos et al., 2020, Breshears et al., 2021, Ciais et al., 2005), etc. Zhao et al. proposed that economic losses caused by heat-related labor productivity losses are projected to account for 0.31% (0.14–0.5%, RCP2.6) to 2.6% (1.4–4%, RCP8.5) of global GDP in 2100 (Zhao et al., 2021). Another recent study shown that this economic losses increase by 0.28%–0.61% of the GDP for each 1 °C rise in temperature in China (Liu et al., 2021). Although the above macro level studies have conducted meaningful investigations on the historical and future changes in regional heat waves, the future pattern of global heat waves remains unclear (Wang et al., 2020, Yu et al., 2021, Perkins-Kirkpatrick and Lewis, 2020). Additionally, comparison and verification of the results derived from different data sources is conducive to establishing the confidence of capturing heat waves (Yu et al., 2021, Dong et al., 2021, Sun et al., 2018). And the socioeconomic exposure, as well as the potential risk of heat wave also need further study.

This study focuses on the historical and future changes of global heat waves, as well as the socioeconomic exposure and risks induced by future heat waves. The specific questions are: (1) the spatiotemporal variation of global heat waves' frequency, duration, and intensity, etc. in history (1971–2020) and in the future (2021–2100). For example, their spatial distribution and temporal variation tends; (2) the exposure population and economies of global heat waves in different regions, periods, and socioeconomic conditions; (3) the potential heat wave risk with socioeconomic inequality and adaptability considered in the future. For our research goals, we employed 3 historical hourly climate data of CRU JRA, ERA5, and GLDAS, as well as 15 CMIP6 GCMs (Global Climate Models) modeled daily data under three SSPs (Shared Socioeconomic Pathways) to produce a longtime global heat wave record dataset and investigate the spatiotemporal variation of global heat waves, the dataset and source code are publicly available at https://doi.org/10.6084/m9.figshare.17075660.v6. Moreover, global population and GDP projections consistent with SSPs are used to estimate socioeconomic exposure and risks induced by future heat waves. This study is of great significance for our humans to understand and deal with the worldwide intensifying heat waves, which may be one of the most impressive climate extremes in a warming future.

2. Material and methods

2.1. Data

2.1.1. CRU JRA, ERA5, and GLDAS hourly climate data

Multi-source historical climate data of CRU JRA, ERA5, and GLDAS from 1971 to 2020 are used to generate yearly heat wave records. CRU JRA (https://archive.ceda.ac.uk/) dataset is a 6-hourly and 0.5° grided global time series of 10 meteorological variables from January 1901 to present produced by the Climatic Research Unit (CRU). The dataset is constructed by downloading data from the Japanese Reanalysis data (JRA) and quality controlled by CRU (Kobayashi et al., 2015, Harris et al., 2014). ERA5 (https://www.

ecmwf.int/en/forecasts/datasets/reanalysis-datasets/era5/) is the fifth-generation high resolution (0.25°) ECMWF (European Centre for Medium-Range Weather Forecasts) reanalysis for many atmospheric, ocean-wave and land-surface quantities. It assimilates model data with observations across the world into a globally complete and consistent dataset. ERA5 datasets have been assessed by the Evaluation and Quality Control (EQC) function of C3S (Copernicus Climate Change Service) independently of the data supplier for data usability and reliability (Hersbach et al., 2020). Using satellite and ground observational data, as well as advanced land surface modeling and data assimilation techniques, GLDAS (Global Land Data Assimilation System, https://ldas.gsfc.nasa.gov/gldas/) is developed to generate optimal global hourly fields of land surface states and fluxes in near–real time and high resolution (0.25°) from 1948 to present. The high-quality land surface fields provided by GLDAS has supported several current and proposed weather and climate prediction, water resources applications, and water cycle investigations. (Rodell et al., 2004, Houser, 2003).

In this study, hourly temperature of CRU JRA, ERA5, and GLDAS from 1971 to 2020 is resampled as daily mean, minimum and maximum temperature firstly. Next, daily temperature is used to generate high temperature thresholds. Then, daily temperature and high temperature thresholds are employed to calculate yearly heat wave records. The detailed data processing process can be accessed in method section.

2.1.2. CMIP6 daily modeled data

Historical (1971–2014) and future (2015–2100) daily modeled data of 15 CMIP6 (Climate Model Intercomparison Project 6) GCMs are employed to generate and validate future heat wave records. The source data is accessed at CDS (Climate Data Store) CMIP6 climate projections catalogue entry (https://cds.climate.copernicus.eu/cdsapp#!/dataset/projections-cmip6?tab = overview), which provides daily and monthly global climate projections data from numerous experiments, models and time periods computed in the framework of CMIP6. 15 GCMs are selected based on the following the following three conditions. First, the temporal resolution is daily. Second, at least four experiments of historical, SSP1 2.6, SSP2 4.5 and SSP5 8.5 are included. At last, the temporal range must include 1971 to 2100. The selected 15 CMIP6 GCMs are shown in Table 2.

Historical (1971–2014) modeled daily maximum temperature of 15 CMIP6 GCMs are used to generate high temperature thresholds and validate predicted future heat waves, and future (2015–2100) data under SSP1 2.6, SSP2 4.5, and SSP5 8.5 are used to produce future heat wave records (See Section 2.2.1). SSPs delineates the different trajectories of future socioeconomic systems and can reflect the correlation between socioeconomic development patterns and climate change risks (WENG et al., 2020). SSPs and RCPs (Representative Concentration Pathways) represent the socioeconomic scenarios and climate scenarios in the new scenario framework proposed by ICPP in 2010 respectively (Moss et al., 2010). We used three SSPs to represent high, medium, and low emission scenarios. The processing process of daily temperature are similar as hourly records.

2.1.3. Global spatial population and GDP scenarios

We used population projections of spatial population scenarios under SSP1, SSP2, and SSP5 to assess future population heat wave exposure (https://www.cgd.ucar.edu/iam/modeling/spatial-population-scenarios.html). Spatial population scenarios are a new set of global, spatially explicit (1/8° grided) population scenarios that are consistent with SSPs, covering the period 2010–2100 in intervals of 10 years. It is produced by parameterized gravity-based downscaling model and quantitatively consistent with national population and urbanization projections for the SSPs, as well as assumptions in the SSP narratives regarding spatial development patterns (Jones and O'Neill, 2016). Gridded GDP Projections summarize global GDP scenarios in 1/12° grids from 2010 to 2100 by 10 years interval, which are estimated by downscaling GDP projections under five SSPs (Murakami et al., 2021).

Socioeconomic exposure induced by heat waves are obtained by the statistics of population and GDP in the heat wave area (Cai et al., 2021). According to the risk triangle theory (Kazmierczak and Cavan, 2011), they are also employed as the source of exposure and vulnerability in the assessment of potential heat wave risk, respectively.

2.2. Methods

2.2.1. Heat wave definition and identification

Generally, a hot weather process that lasts for several consecutive days is defined as a heat wave. Thus, the definition of heat wave involves two main parameters, high temperature threshold and duration threshold (Perkins, 2015). Currently, there are no unified standard for heat waves (Yin et al., 2020, Raei et al., 2018, Gao et al., 2015). The World Meteorological Organization (WMO) suggests that a high temperature weather process exceeding 32 °C and lasting for more than three days is a heat wave event (Wang et al., 2018). In most areas of China, the standard for high temperature is 35 °C (Chen and Li, 2017). Constant threshold and percentile threshold are mainly used in determining high temperature thresholds (Huang et al., 2010, Williams et al., 2012, Stefanon et al., 2012, Vautard et al., 2013). Some comprehensive heat wave indexes, such as Excess Heat Factor (EHF) (Perkins and Alexander, 2013) and Standardized Heat Index (SHI) (Raei et al., 2018) are also used in recent studies. Considering the method universality and data availability, we used a combination of constant threshold and percentile threshold to define heat waves.

Constant threshold determines a fixed high temperature standard over the entire area and period, and heat wave events are defined with the corresponding high temperature and duration threshold. While in the long-term adaptation process, the suitable temperature range of residents may vary in different regions (Xu et al., 2020, Yin et al., 2019), constant threshold is suggested to be used in a smaller spatial extent. Percentile threshold localizes high temperature standard based on local climatology both temporally and spatially. More specifically, temperature threshold for each calendar day and each grid is specified as an upper-tail percentile threshold of the Probability Distribution Function (PDF) constructed by long-term daily temperature series of n-days centered on each calendar day (Vautard et al., 2013, Panda et al., 2017). It is useful in detecting warm spells, which may appear even with low temperatures.

Consequently, it is necessary to add constraints in defining heat wave events.

In this study, we use combined threshold to detect heat waves. Heat waves are defined as daily maximum temperature exceeds both constant threshold (35 °C) and percentile threshold (90% with a 15-days' time window) for more than three consecutive days. Here, the daily percentile threshold was determined from the 90th percentile of the daily maximum temperature series in a 15 days' time window centered on that day from 1971 to 2014 ($n = 44 \times 15$, Equation (1)). The time range from 1971 to 2014 was determined based on the available range of CMIP6 historical data. Combined threshold not only considers the regional climatology, but also avoids the detection of anomalously warm spells with low absolute temperatures as heat waves, even though it may adversely affect human health (Burke et al., 2018). So it can be used to detect heat wave on a global scale (Yin et al., 2020). We used 8 attributes to characterize the frequency, duration, intensity, and temporal range of heat waves, which are shown in Table 1.

$$U_d = \bigcup_{1971}^{2014} \bigcup_{d-7}^{d+7} T_{max} \quad (1)$$

Where, U_d is the set of daily maximum temperatures (T_{max}) for which the percentile threshold of the day (d) is calculated.

An overview of materials, methods, and outputs of this study is shown in Fig. 1. The workflow can be divided into two parts: heat wave records part and heat wave exposure / risk part. In the first part, historical and future climate data are used to generate historical and future heat wave records respectively. For historical heat wave records, hourly temperature is resampled to daily temperature records firstly. Then, for each calendar day d, a collection of daily temperature from 1971 to 2014 over a window of n days centered around the calendar day d is constructed, and percentile threshold is defined as upper tail threshold of the collection. Finally, accompanying with constant threshold and duration threshold, heat waves are defined as daily temperature exceeding both constant threshold and percentile threshold, and lasting more than duration threshold days.

Future heat wave records are generated in similar way but with two differences. First, future climate data is already at daily level and does not need to be resampled. Second, relative high temperature thresholds are generated from the historical (1971–2014) modeled data of the corresponding GCMs. For the second part, heat wave records are firstly unified to the same spatial resolution of population and GDP data, and exposure is calculated with the summary of population or GDP in area with heat waves. Potential heat wave risk is evaluated using the combination of heat wave records, population, and GDP, according to the risk triangle theory.

2.2.2. GHWT: Global heat wave toolbox

Considering the convenience of the reuse of code and datasets, a visualized python-based Global Heat Wave Toolbox (GHWT) is developed. GHWT has three function modules of calculating daily temperature, high temperature threshold and yearly heat wave based on multiple data sources. The yearly heat wave calculation module has 8 outputs, corresponding with 8 characteristics of heat waves in Table 1. GHWT allows users to customize some key parameters to suit different needs of datasets, such as statistic method and high temperature threshold, etc. The GUI (Graphical User Interface) of the toolbox is shown in Fig. 2.

2.2.3. Socioeconomic exposure and risks induced by future heat waves

Exposure refers to the inventory of elements in an area in which hazard events may occur (Cardona, 1990). Existing studies usually use the product of population / GDP and frequency / duration of disaster events to represent socioeconomic exposure (Feng et al., 2021, Wang et al., 2020, Lehner and Stocker, 2015). In this study, exposure is quantified at two levels: scale and intensity. Exposure scale is used to identify populations and economies exposed to different intensities of heat waves, which is the sum of the population or GDP of the heat wave area. And exposure intensity is quantified by the product of population / GDP and heat wave duration. Specifically, heat waves are resampled to the same spatial resolution as the population and GDP data. Next, heat waves and population data, as well as GDP data are spatially superimposed to quantify socioeconomic exposure. We used "Raster Calculator" tool of ArcGIS to perform sum (exposure scale) and product (exposure intensity) operations. As population and GDP data are all decadal interval data, heat wave data is averaged using corresponding decadal data.

We used the hazard-exposure-vulnerability risk evaluation model to assess the potential heat wave risk (Kazmierczak and Cavan, 2011). Heat wave risk is the probability of harmful consequences resulting from interactions among heat wave hazard (the possible future occurrence of heat waves), exposure (total population, its livelihoods and assets where heat waves may occur) and vulnerability (the propensity of exposed elements to suffer adverse effects when impacted by heat waves) (Cardona et al., 2012). We used HWD, population and GDP to represent heat wave frequency, exposure, and vulnerability, respectively. And heat wave risk is the normalized value of their product, as shown in Equation (2).

Table 1
Abbreviation and definition of heat wave characteristics.

Heat wave characteristic	Abbreviation	Definition
Heat wave frequency	HWF	Number of yearly heat wave events
Heat wave duration	HWD	Number of yearly heat wave days
Heat wave average duration	HWAD	Average duration of each heat wave event (HWD / HWF)
Heat wave maximum duration	HWMD	Duration of longest heat wave event
Heat wave average temperature	HWAT	Mean temperature of heat wave days
Heat wave maximum temperature	HWMA	Maximum temperature among heat wave days
Heat wave start date	HWSD	Start date of the first heat wave event
Heat wave end date	HWED	End date of the last heat wave event

Table 2
Average recognition rate, RMSE (HWF), and RMSE (HWD) for 15 GCMs.

GCM	Recognition rate	RMSE (HWF)	RMSE (HWD)
MIROC6	58.03	2.97	16.66
KIOST-ESM	56.80	3.43	20.98
MRI-ESM2-0	54.19	2.22	12.26
CNRM-ESM2-1	52.35	2.30	12.40
CMCC-ESM2	51.77	2.23	12.16
INM-CM5-0	50.27	2.11	11.39
EC-EARTH3-VEG-LR	50.10	2.10	11.76
INM-CM4-8	50.05	2.09	11.49
AWI-CM-1–1-MR	49.30	2.25	12.54
CNRM-CM6-1	48.69	2.23	12.32
NORESM2-MM	47.72	2.33	12.58
GFDL-ESM4	45.62	2.04	10.62
ACCESS-CM2	43.88	2.25	12.35
MIROC-ES2L	42.02	2.48	13.23
MPI-ESM1-2-LR	40.20	2.14	11.81

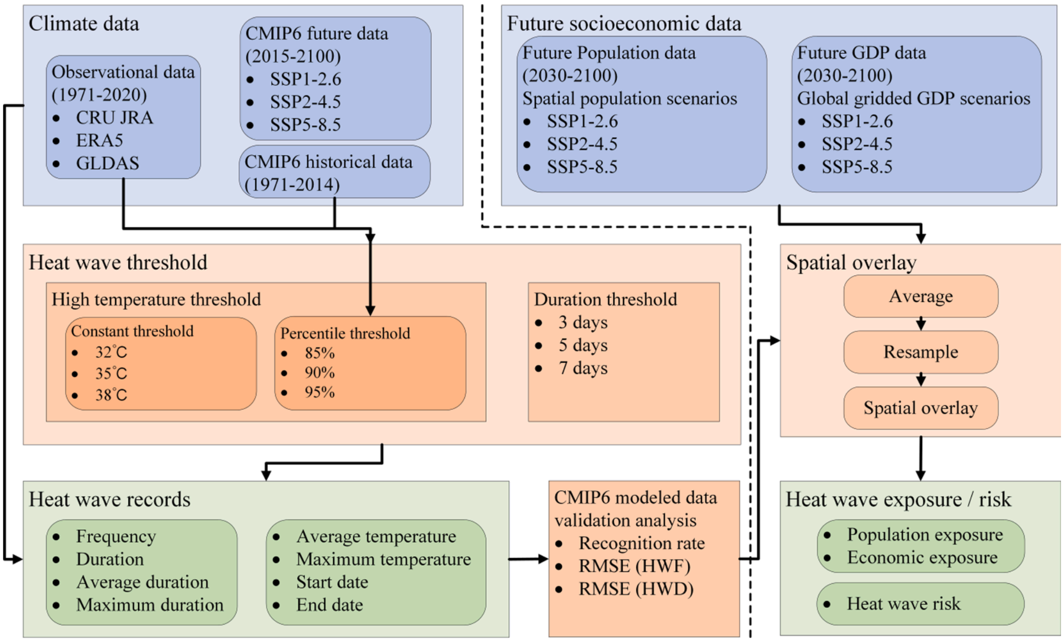

Fig. 1. An overview of materials, methods, and outputs of this study.

$$Risk = Hazard \times Exposure \times Vulnerability \quad (2)$$

3. Results

3.1. Spatial distribution of historical heat waves

Fig. 3 maps the average state of historical heat waves derived from CRU JRA, ERA5, and GLDAS. Generally, all three datasets reveal similar heat wave spatial pattern, with GLDAS detected more heat waves with longer duration. The results show that except for high latitudes (latitude greater than 60°), high elevations and some coastal areas, heat waves have visited about 45% (±3%) of the global land area (excluding Antarctica). North Africa, North Australia, South Asia, and the Arabian Peninsula are detected as high heat wave area, where experience more than three heat waves with total duration over 15 days annually. In the rest of the heat wave region, heat waves are usually less than three times a year, with a total duration of less than 15 days (Fig. 3a and 3b). Extreme heat wave intensity is detected in the Arabian Peninsula, North Africa, India and Australia, where the average temperature during heat waves is usually above 39 °C (Fig. 3c). We also discussed the temporal characteristics of heat waves (Fig. 3d and 3e). The start time and end time of heat wave are generally distributed in layers. In NH, the start of the heat wave is delayed by two months for every 20°increase in latitude. For example, India's first heat wave usually occurs in March to April, while Russia's first heat wave usually occurs in July to August.

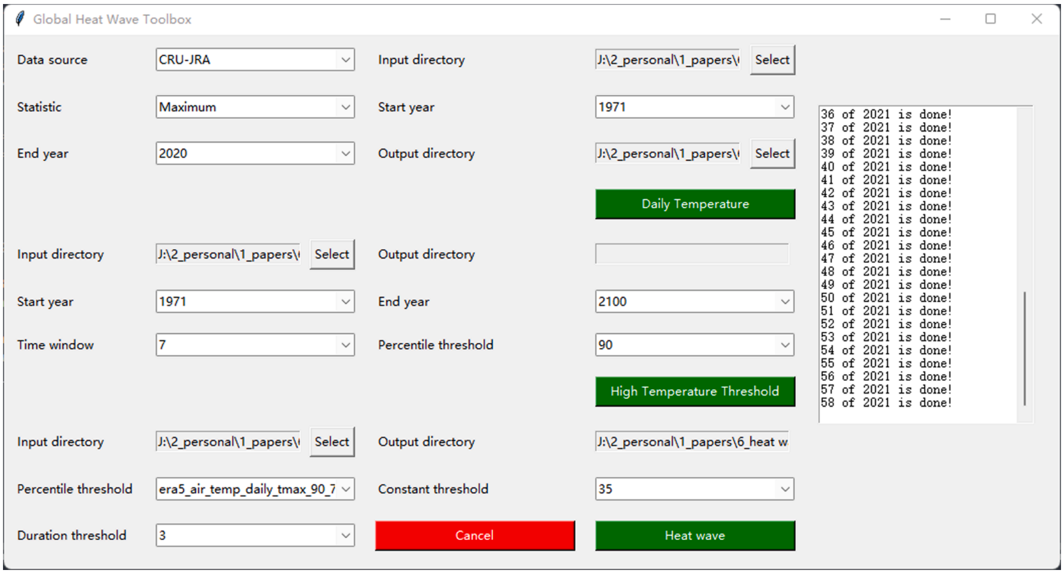

Fig. 2. GUI of GHWT.

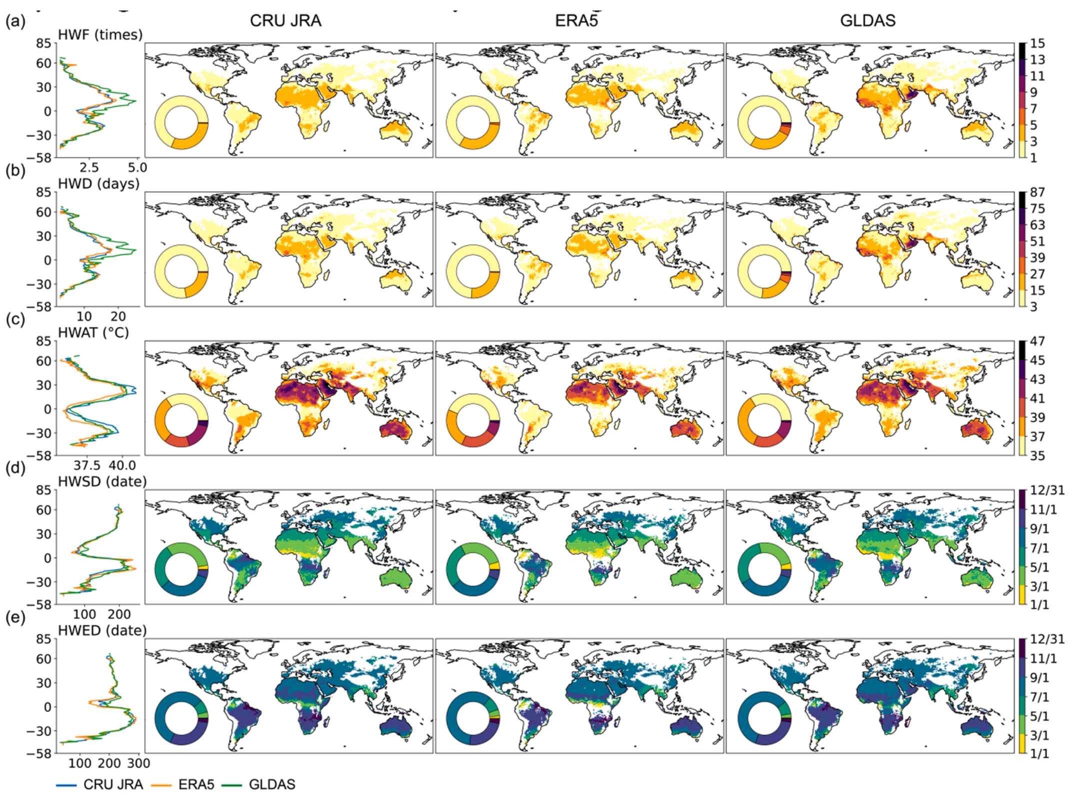

Fig. 3. Average state of historical heat waves derived from CRU JRA, ERA5, and GLDAS for (a) HWF, (b) HWD, (c) HWAT, (d) HWSD, and (e) HWED. The curves on the left demonstrate the mean value on corresponding latitude for three data sources respectively. The rings show the proportion of different value ranges.

The last heat wave usually ends in August, the end of boreal summer.

3.2. Observed increasing trends in historical heat waves

We further investigated the changing direction and intensity of regional heat waves. Fig. 4 demonstrates the slope and significance of historical heat waves derived from three data sources. Linear regression is practiced if heat waves occurred in more than 30 of all 50 years (1971–2020) for each grid cell. Apparently, heat wave frequency, duration, and intensity have significant (P value less than 0.05) increasing trends. For HWF and HWD, over 90% heat wave areas that passed the significance test have increasing trend, with a rate of less than 3 times and 20 days per decade. North Africa and the Arabian Peninsula are identified as rapid heat wave growth region (Fig. 4a and 4b). Interestingly, HWAT has declining trend in about 20% heat wave areas that passed the significance test, including North Africa and some of Australia. Considering the increase of HWD, this may be due to the expansion of the heat waves to some cooler dates (Fig. 4c). The advance of HWSD and delay of HWED are drastic in North Africa, the Arabian Peninsula, India, and Australia, with less than three days per year, which is consistent with the increase in HWD (Fig. 4d and 4e). If significance is ignored, heat wave increasing trends will be detected in more areas.

The yearly changes of 6 heat wave characteristics are shown in Fig. 5. Generally, global mean heat wave frequency and duration have doubled from 1971 to 2020, with a growth rate of 0.4 times and 2 days per decade. HWF have increased from 2 times in 1971 to 4 times in 2020, and HWD have increased from 9 days to 18 days. HWAD also has a weak growth trend. As heat wave spread to more dates with relatively low temperature, HWAT have a decreasing trend. Additionally, HWSD is advancing and HWED is postponing, with a rate of 5 days and 7 days per decade. Compared with 1971, HWSD has been advanced by 20 days and HWED has been delayed by 40 days.

3.3. Projected spatial pattern of future heat waves

To establish the confidence of CMIP6 GCMs in predicting future heat waves, we evaluated the performance of 15 GCMs in capturing historical heat waves using recognition rate, RMSE (HWF), and RMSE (HWD). Specifically, we first generated heat wave records using historical (1971–2014) GCMs data and compared them to the mean of heat wave records from three observational datasets (CRU JRA, ERA5, and GLDAS) during the same period. The recognition rate is the proportion of the number of heat wave pixels identified by GCMs data to the total number of heat wave pixels identified by observation data. RMSE is the root mean square error of the difference in heat wave frequency (duration) between two sets of data. According to the evaluation results in Figure S1 and Table 2, heat wave

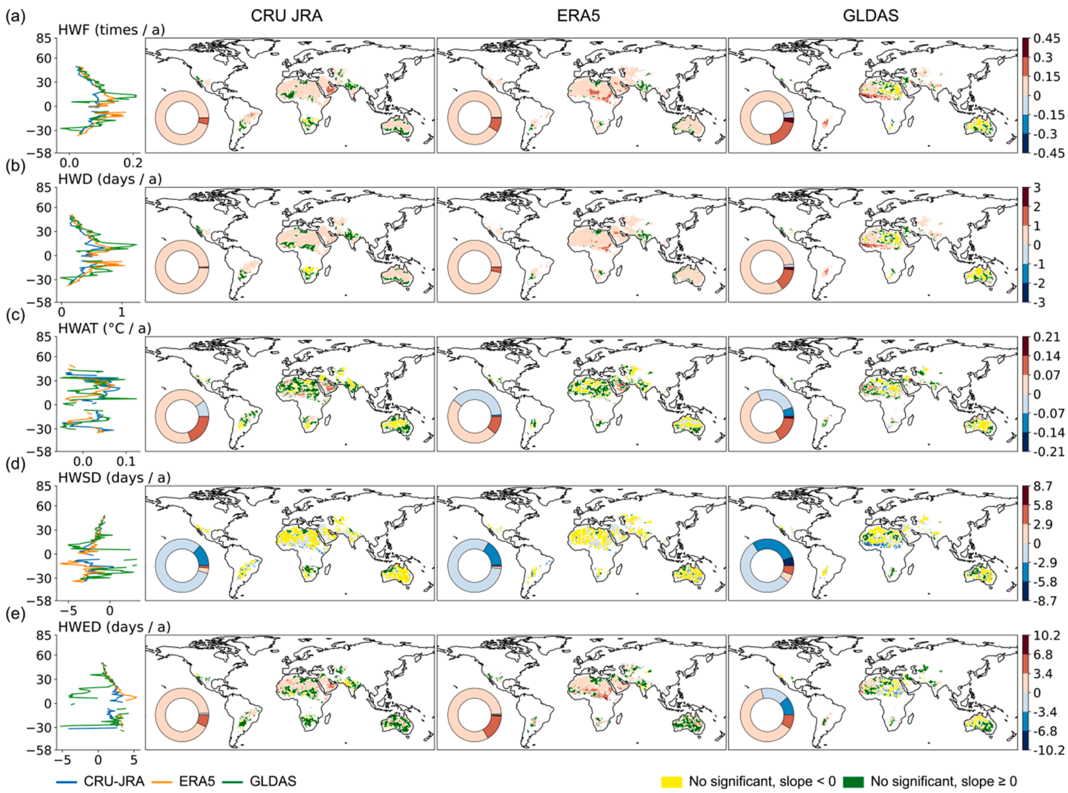

Fig. 4. Slope and significance of historical heat waves derived from CRU JRA, ERA5, and GLDAS for (a) HWF, (b) HWD, (c) HWAT, (d) HWSD, and (e) HWED. Yellow and green represent no significant areas (P value greater than 0.05).

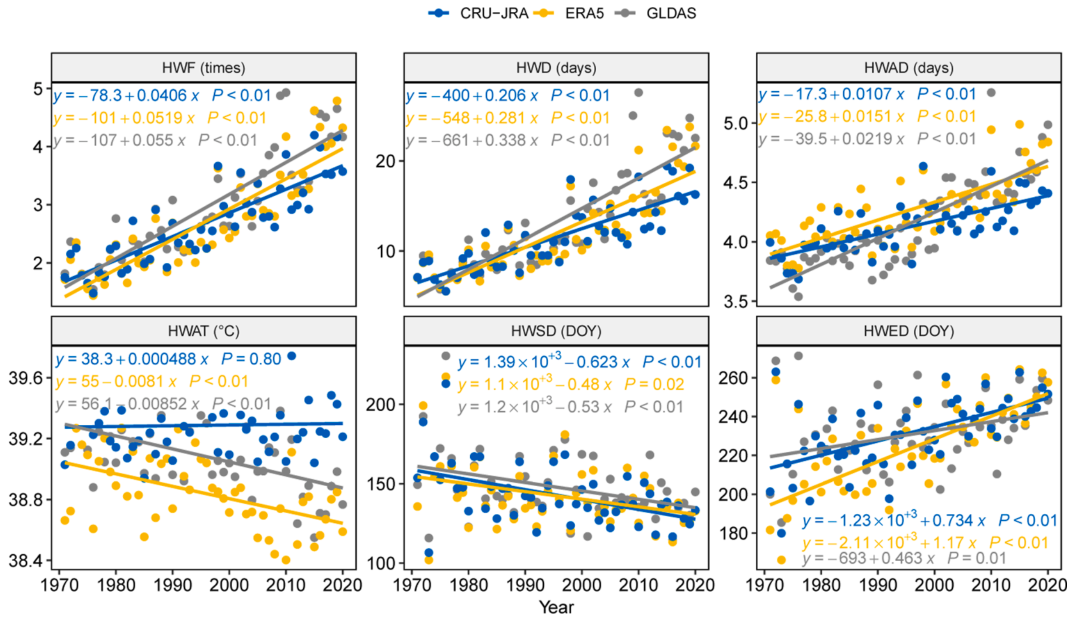

Fig. 5. Mean annual HWF, HWD, HWAD, HWAT, HWSD, and HWED derived from CRU JRA, ERA5, and GLDAS.

recognition rate and RMSE increased chronologically. The average recognition rate of all GCMs is above 40%, while the RMSE of HWF and HWD is between 2.04 and 3.43 and 10.62–20.98.

15 GCMs were employed to predict the average state of future heat waves under 3 SSPs. According to Fig. 6, From SSP1 2.6 to SSP2 4.5 and SSP5 8.5, due to looser emission reduction measures and more severe global warming, heat wave spatial extent is increasing, which indicates more novel areas are likely to experience heat waves. For example, under SSP5 8.5, heat waves may spread to the

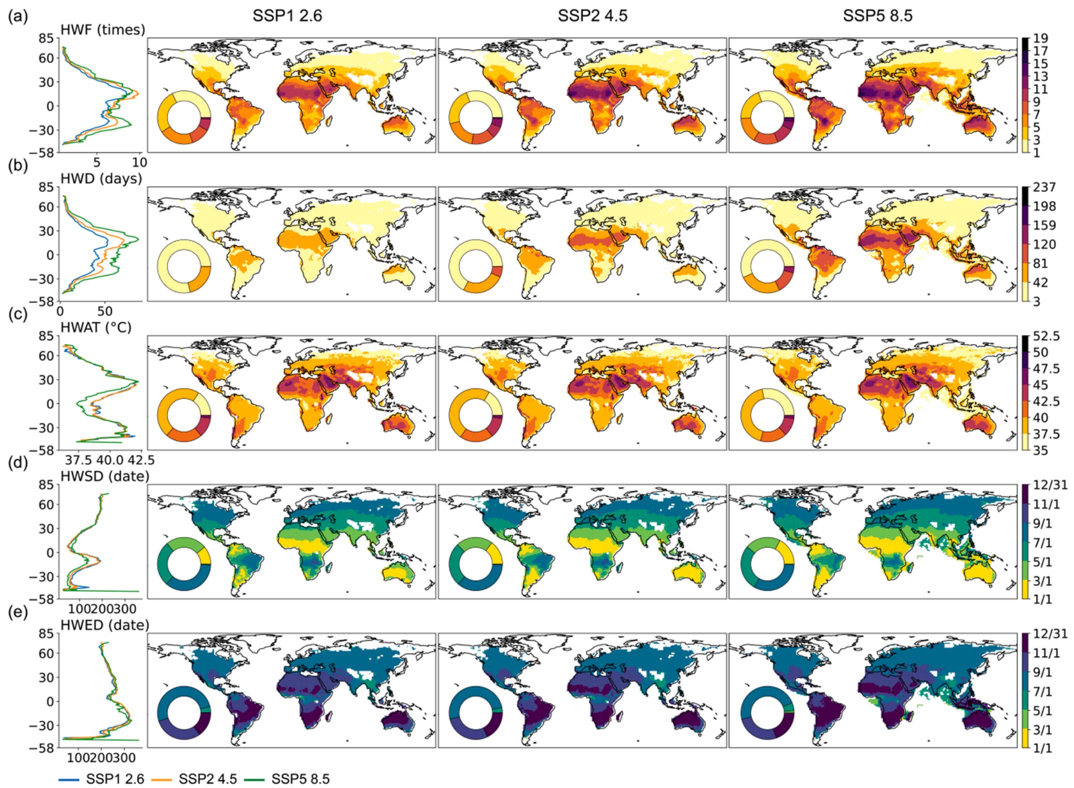

Fig. 6. Average state of future heat waves under SSP1 2.6, SSP2 4.5, and SSP5 8.5 for (a) HWF, (b) HWD, (c) HWAT, (d) HWSD, and (e) HWED.

whole of Canada and Russia. The proportion of high HWF and HWD is also increasing, which means more regions may suffered from more serious heat waves if no climate mitigation measures are practiced, especially in North Africa, the Arabian Peninsula, Australia, and Brazil. In the future, HWF in more than 70% and HWD in more than 30% (±10%) of heat wave areas may exceed 5 times and 42 days a year respectively, which is a sharp increase compared to the historical state. Additionally, consist with the increase in HWD, HWSD is earlier and HWED is later under SSP2 4.5 and SSP5 8.5. Compared to historical records, HWSD and HWED in North Africa, Australia, and Brazil was advanced or delayed for about one month (Fig. 6d and 6e).

3.4. Continuous increasing trends in future heat waves

We highlighted the increase of heat waves in a warmer further. Fig. 7 shows the linear regression results of further heat waves under 3 SSPs. Linear regression is practiced if heat waves were detected in 51 of all 86 years (2015–2100) for each grid cell. From SSP1 2.6 to SSP5 8.5, areas passing significance test is increasing, as well as the proportion of slope less than 0 for HWSD, and slope over 0 for the other four heat wave characteristics, which indicates heat wave area, frequency, duration, and intensity with significantly increase in the future if no climate mitigation measures are taken. In contrast, under SSP1 2.6, the linear regression results of a fair number of heat wave areas failed to pass significance test, which shows that climate mitigation measures will effectively curb the increasing trend of heat waves. Under SSP2 4.5, heat wave will still experience a slow but significant increase. This means if we continue the current emission pathway, heat waves will increase further. North Africa, Australia, and Brazil are identified as rapid heat wave growth area. Additionally, the average growth rate of global HWF, HWD, and HWAT under SSP2 4.5 and SSP5 8.5 may be 2–3 times and 3–5 times of that under SSP1 2.6, respectively. The growth trend of heat wave will be greatly slowed down under SSP1 2.6, while under SSP2 4.5 and SSP5 8.5, heat waves may continue or even increase sharply (Table 3).

Fig. 8 further demonstrated the yearly changes of future heat waves among 6 GCMs. 6 GCMs were chosen because of their better heat wave capturing performance (Table 2). Specifically, the recognition rate of heat wave is above 50%, and they have the lowest RMSE. Under SSP1 2.6, heat waves increase smoothly in the next 30 years, and almost all GCMs predicted the downward trend of heat waves after 2050. Under SSP2 4.5, heat waves will continue to increase, but in most GCMs, the growth trend of heat waves will slow down. While under SSP5 8.5, heat waves will increase sharply and faster. These emphasizes the importance of positive emission pathways in curbing the increase of heat waves.

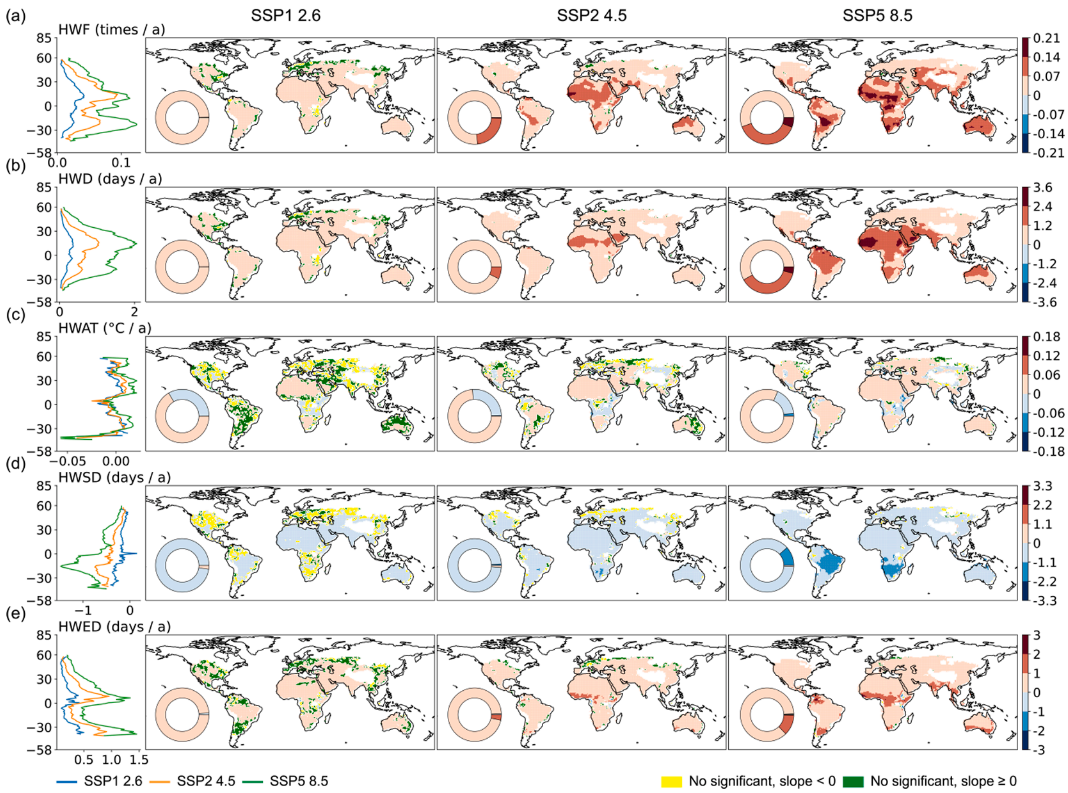

Fig. 7. Slope and significance of the linear regression results of global heat waves from 2021 to 2100 under SSP1 2.6, SSP2 4.5, and SSP5 8.5 for (a) HWF, (b) HWD, (c) HWAT, (d) HWSD, and (e) HWED.

Table 3
Global statistical results of slope under 3 SSPs.

Heat wave characteristic	SSP1 2.6	SSP2 4.5	SSP5 8.5
HWF (times / a)	0.02	0.05	0.07
HWD (days / a)	0.2	0.5	1.09
HWAT (°C / a)	0.01	0.03	0.09
HWSD (days / a)	−0.19	−0.36	−0.6
HWED (days / a)	0.19	0.37	0.58

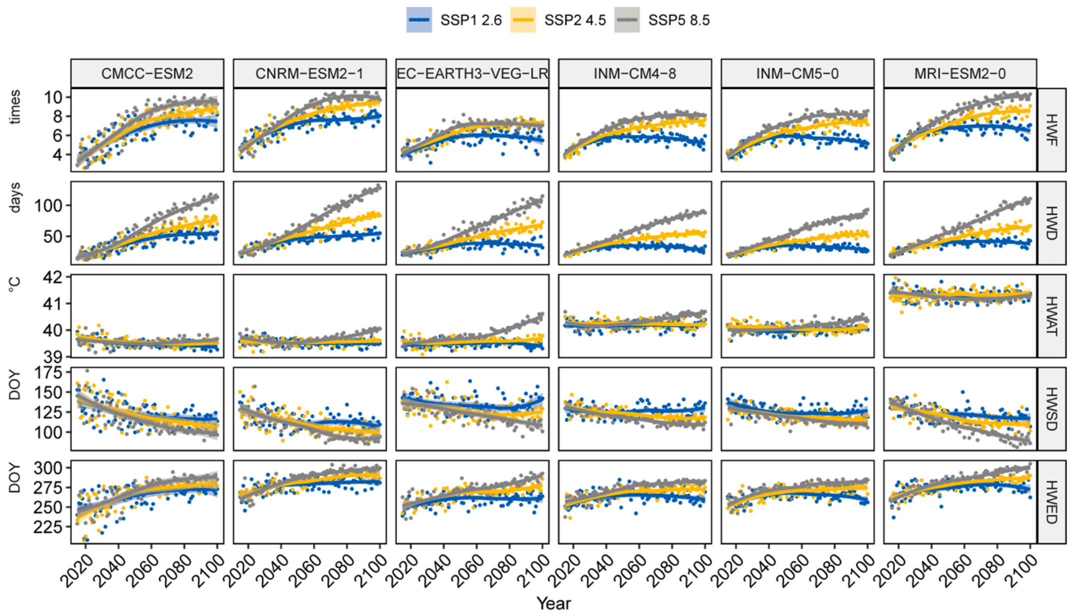

Fig. 8. Yearly change of future heat waves among 6 GCMs under SSP1 2.6, SSP2 4.5, and SSP5 8.5 for HWF, HWD, HWAT, HWSD, and HWED.

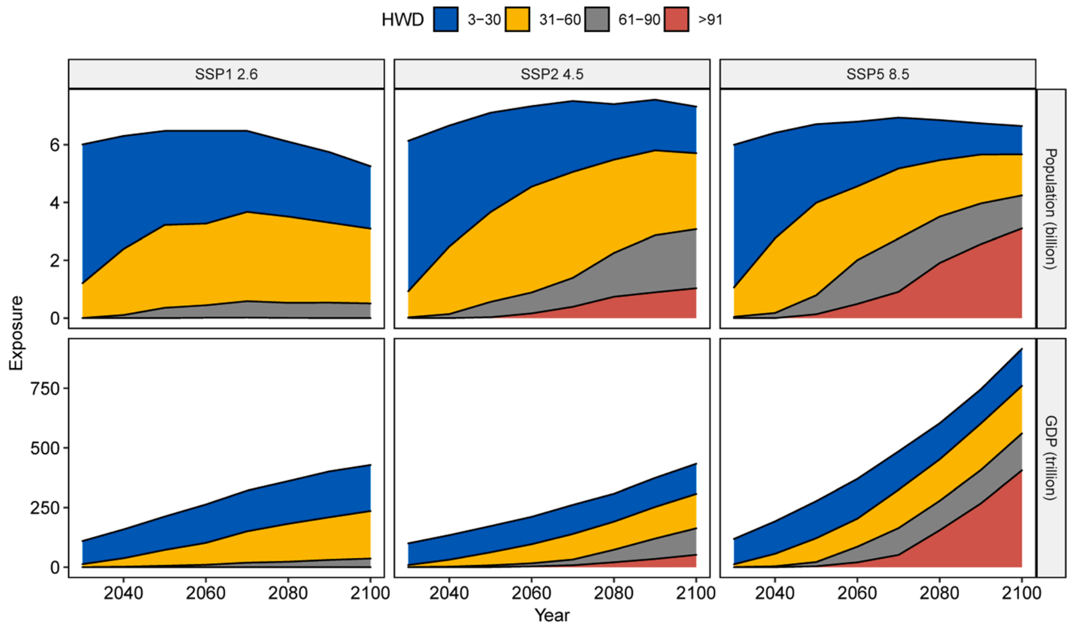

Fig. 9. Population and economic exposure scale under heat waves with different duration in the future under SSP1 2.6, SSP2 4.5, and SSP5 8.5.

3.5. Assessment of global heat wave exposure and risks

Fig. 9 shows the population and economic exposure scale under heat waves with different duration in the future under 3 SSPs. Generally, compared to SSP1 2.6, more people may be affected by heat waves with longer duration under SSP2 4.5, while population exposure under SSP5 8.5 is lower than SSP2 4.5. This may be due to human reduction and migration caused by resource and environmental problems under high emission pathways. Under SSP2 4.5, there may be about 6.13 billion people exposed to heat waves in 2030, accounting for 75.67% of the global population. And this figure will increase to 7.32 billion and 82.65% in 2100. Additionally, 3.08 billion people may expose to heat waves with duration over 60 days in 2100. Economic exposure may have a chronological increase. Due to the positive, clean, and sustainable development model, there may be a larger economic scale under SSP1 2.6. Consequently, economic exposure under SSP1 2.6 is usually higher than that under SSP2 4.5. Under SSP2 4.5, economic exposure may reach $99.87 trillion in 2030 and $433.37 trillion in 2100, accounting for 71.39% and 82.23% of the total global economy in that year.

Countries with the highest population and economic exposure scale to future heat waves under SSP2 4.5 are mapped in Fig. 10. On the ground of huge population and heat wave area, India may have the highest population exposure and far more than other countries. Under SSP2 4.5, 1.42 to 1.48 billion Indians may be exposed to heat waves in the remaining two 40 years of the 21st century. Some populous African, Asian, and American countries also have high population exposure, such as Pakistan, Nigeria, Bangladesh, China, and the United States. Due to the poor economic level and medical conditions in most of these countries, they may face serious health pressure caused by future heat waves. India may also suffer from the highest economic exposure. Tens of trillions of dollars economy may be exposed to heat waves. Under SSP2 4.5, $21.26 trillion economies will be exposed to heat waves in 2030 to 2060, and this figure will increase to 58.32 trillion in 2070 to 2100. The world's two largest economies, the United States and China, will also play an important role in heat wave economic exposure. Consequently, heat waves will pose a serious threat to the global economy in the future.

The socioeconomic exposure intensity and potential risk of global heat waves are mapped in Fig. 11. India, Eastern China, Eastern United States, the Arabian Peninsula, Southern Europe, and Central Africa were identified as high population exposure areas. From

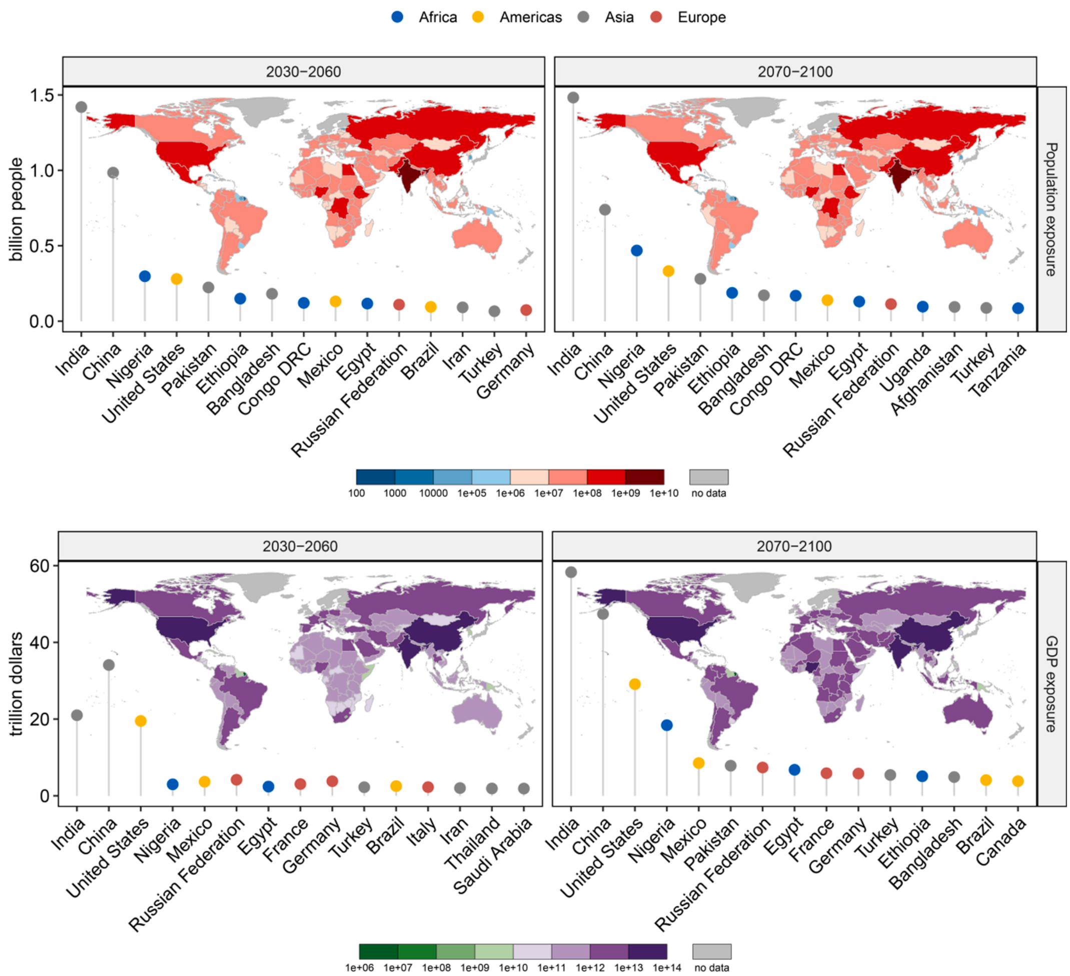

Fig. 10. Population and economy exposed to heat waves by countries for 2030 to 2060 and 2070 to 2100 under SSP2 4.5.

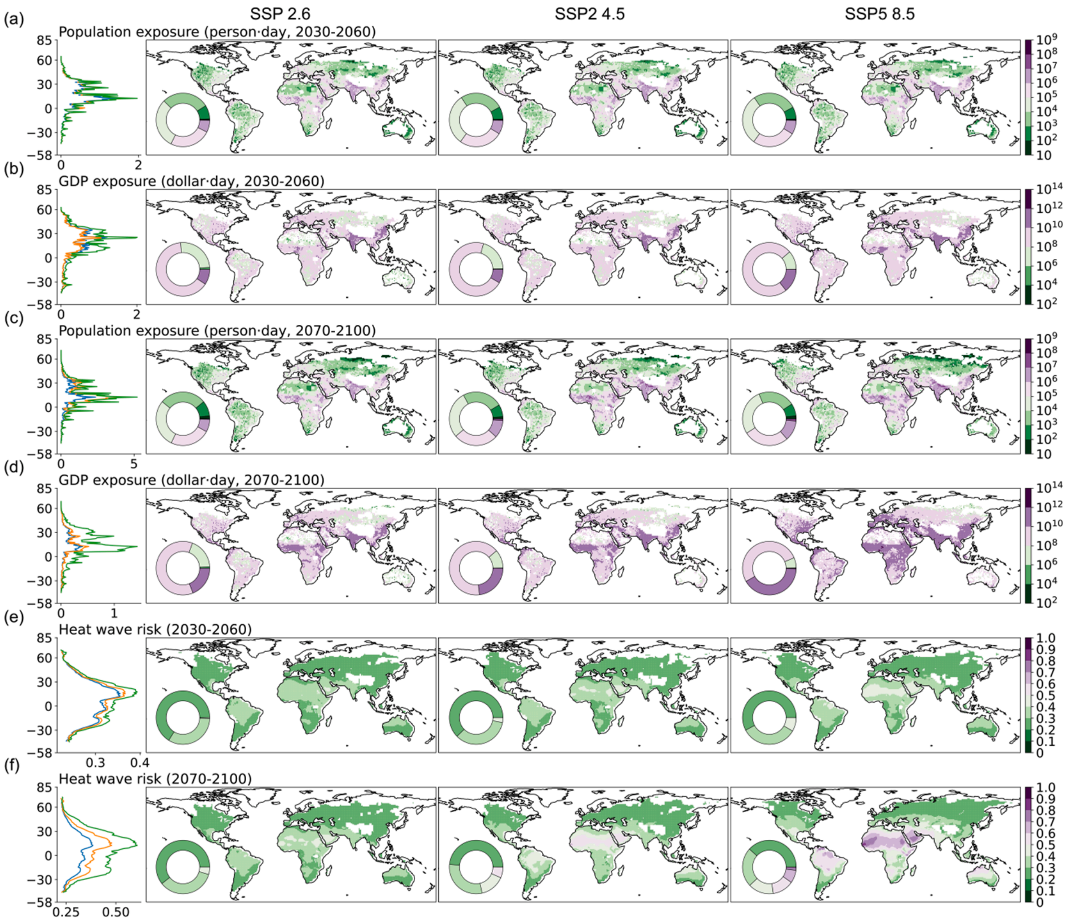

Fig. 11. Socioeconomic exposure and potential risk for 2030 to 2060 and 2070 to 2100 under 3 SSPs: (a) Population exposure for 2030 to 2060; (a) Population exposure for 2070 to 2100; (c) GDP exposure for 2030 to 2060; (d) GDP exposure for 2070 to 2100; (e) heat wave risk for 2030 to 2060; (f) heat wave risk for 2070 to 2100.

SSP1 2.6 to SSP5 8.5, economic exposure may increase significantly. India, Eastern China, Eastern United States, and Western Africa may face higher economic exposure. Between the remaining two 40 years of the 21st century, economic exposure will increase by an order of magnitude. For heat wave risk, the difference between three SSPs is small from 2030 to 2060, while the difference is large from 2070 to 2100. This means that under the high emission pathway, more regions may face higher heat wave risk at the end of the 21st century. Given the frequent heat waves, dense population, or relatively low economic level in North Africa, the Arabian Peninsula, Pakistan, India, Brazil and northern Australia, the risk of heat waves is higher in these regions.

4. Discussion

Our conclusions are basically consistent with relevant studies (Dong et al., 2021, Sun et al., 2018, Yu et al., 2021, Dosio et al., 2018), which also reveals the continuous growth trend of historical and future heat waves, as well as the importance of taking emission reduction measures. We investigated the temporal characteristics of heat waves, such as their start and end dates, which were usually not noticed before. In addition, we show the population and economy exposed to different levels of heat waves in time series, which is of great significance to deal with future extreme climate. We found some interesting points in our study. Firstly, HWF and HWD increased as expected, while HWAT has a significant downward trend with global warming from 1971 to 2020. The reason could be heat waves have expanded to more regions and dates, and temperatures in these regions and dates are relatively low, even if they have reached the standard of heat wave. Secondly, the middle and low latitudes ($10-30^{\circ}$N and $10-30^{\circ}$S) are high heat wave growth regions, while the growth in the equatorial region (10°S $-$ 10°N) is usually insignificant or relatively low, especially in island countries such as Indonesia and Philippines. Given the high humidity in these areas, this may be related to atmospheric dynamics and land climate interactions. Next, there is no significant difference in population exposure among 3 SSPs, which means that due to the resource and environmental problems caused by the high emission path, the migration or reduction of population can offset some of the increase of heat waves. At last, the development of socioeconomic level may effectively reduce heat wave risk. For example, compared with India, although China may face high heat wave exposure at the end of the 21st century, its heat wave risk is relatively low in the same latitude region. This is because China's population is expected to decline in 2030 and the economic level will continue to improve, which will lead to lower exposure and stronger adaptability.

Our study also has some limitations. To begin with, severer impacts of dangerous humid heat waves, as well as nighttime and compound heat waves have been reported in recent studies (Yu et al., 2021, Wang et al., 2021, Wang et al., 2020, Baldwin et al., 2019). However, due to the concerns and priorities of this study, we have not taken them into account. Next, we give estimates of heat wave population and economic exposure under 3 SSPs in the future. This can help us understand the scope and scale of the impact of future heat waves. But this can't answer how many deaths and economic losses may be caused by future heat waves, as death is related to more factors such as living and working environment and medical conditions, while economic losses may be caused by labor losses (Roye et al., 2020, Zhao et al., 2021, Liu et al., 2021). Moreover, heat wave vulnerability may be affected by gender, age, working group, education level, medical accessibility, adaptive capacity, and other factors. However, as it is difficult to obtain the forecast data of these factors (working group, education level, medical level) in the coming decades, we used GDP to comprehensively reflect vulnerability, which may lead to uncertainty in the assessment. Additionally, risk is a combination of hazard, exposure, and vulnerability. This means that even though heat wave hazard may continue to increase in the coming decades, the reduction in exposure (increasing working population and decreasing vulnerable populations such as the elderly and children) and vulnerability (improved education, health care and adaptation) may not lead to an increase in the combined heat wave risk (Vittal et al., 2020). Future work should use comprehensive measurements, such as Wet Bulb Global Temperature, and focus on differences in heat-related death among gender, age group and socio-economic level, as well as the influence mechanism of heat wave on economic loss.

5. Conclusions

In this study, we use three historical climate datasets of CRU JRA, ERA5, and GLDAS, as well as modeled climate dataset of 15 GCMs under three SSPs (SSP1 2.6, SSP2 4.5, and SSP5 8.5) to generate longtime global heat wave records from 1971 to 2100. An integrated heat wave calculation toolbox has also been developed. Then we investigate the spatiotemporal variation of global heat waves. Next, global population and GDP projections are employed to estimate socioeconomic exposure and potential risk in heat wave area. We found that heat wave frequency, duration, and intensity have significantly increased in the past 50 years and may continue to increase in the rest of 21st century. Under medium and high emission pathway, heat wavs will continue to increase, billions of populations and trillions of economies may be exposed to future heat waves. While under low emission pathway, the increase in heat waves will slow down significantly, as well as socioeconomic exposure and potential risk induced by heat waves. This highlights the necessity for climate mitigation measures.

CRediT authorship contribution statement

Cong Yin: Conceptualization, Data curation, Formal analysis, Investigation, Methodology, Resources, Software, Validation, Visualization, Writing – original draft. **Yaping Yang:** Conceptualization, Funding acquisition, Project administration, Resources, Supervision. **Xiaona Chen:** Conceptualization, Methodology, Writing – review & editing. **Xiafang Yue:** Resources, Writing – review & editing. **Yangxiaoyue Liu:** Resources, Writing – review & editing. **Ying Xin:** Investigation, Validation.

Declaration of Competing Interest

The authors declare that they have no known competing financial interests or personal relationships that could have appeared to influence the work reported in this paper.

Acknowledgements

This research was funded by Second Tibetan Plateau Scientific Expedition and Research Program (2019QZKK09), Construction and Application Demonstration of a Mountain Disaster Risk Warning Platform Based on Big Data and Artificial Intelligence in the Eastern Edge of the Qinghai-Tibet Plateau (CAS-WX2021SF-0106-03), National Earth System Science Data Sharing Infrastructure and Earth System Science Data Center, Chinese Academy of Sciences (2005DKA32300), and Branch Center Project of Geography, Resources and Ecology of Knowledge Center for Chinese Engineering Sciences and Technology (CKCEST-2021-2-10).

Heat wave records and the source code of Global Heat Wave Toolbox can be accessed at https://doi.org/10.6084/m9.figshare.17075660.v6.

Appendix A. Supplementary material

Supplementary data to this article can be found online at https://doi.org/10.1016/j.crm.2022.100459.

References

Amengual, A., Homar, V., Romero, R., Brooks, H.E., Ramis, C., Gordaliza, M., Alonso, S., 2014. Projections of heat waves with high impact on human health in Europe. Global Planet. Change 119, 71–84.

Baldwin, J.W., Dessy, J.B., Vecchi, G.A., Oppenheimer, M., 2019. Temporally compound heat wave events and global warming: an emerging hazard. Earths Future 7, 411–427.

BASTOS, A., CIAIS, P., FRIEDLINGSTEIN, P., SITCH, S., PONGRATZ, J., FAN, L., WIGNERON, J. P., WEBER, U., REICHSTEIN, M., FU, Z., ANTHONI, P., ARNETH, A., HAVERD, V., JAIN, A. K., JOETZJER, E., KNAUER, J., LIENERT, S., LOUGHRAN, T., MCGUIRE, P. C., TIAN, H., VIOVY, N. & ZAEHLE, S. 2020. Direct and seasonal legacy effects of the 2018 heat wave and drought on European ecosystem productivity. *Science Advances,* 6.

Borg, M.A., Xiang, J.J., Anikeeva, O., Pisaniello, D., Hansen, A., Zander, K., Dear, K., Sim, M.R., Bi, P., 2021. Occupational heat stress and economic burden: A review of global evidence. Environ. Res. 195.

Breshears, D.D., Fontaine, J.B., Ruthrof, K.X., Field, J.P., Feng, X., Burger, J.R., Law, D.J., Kala, J., Hardy, G.E.S., 2021. Underappreciated plant vulnerabilities to heat waves. New Phytol. 231, 32–39.

Burke, M., González, F., Baylis, P., Heft-Neal, S., Baysan, C., Basu, S., Hsiang, S., 2018. Higher temperatures increase suicide rates in the United States and Mexico. *Nature*. Clim. Change 8 (8), 723–729.

Cai, W.J., Zhang, C., Suen, H.P., Ai, S.Q., Bai, Y.Q., Bao, J.Z., Chen, B., Cheng, L.L., Cui, X.Q., Dai, H.C., Di, Q., Dong, W.X., Dou, D.J., Fan, W.C., Fan, X., Gao, T., Geng, Y., Guan, D.B., Guo, Y.F., Hu, Y.X., Hua, J.Y., Huang, C.R., Huang, H., Huang, J.B., Jiang, T.T., Jiao, K.D., Kiesewetter, G., Klimont, Z., Lampard, P., Li, C.X., Li, Q.W., Li, R.Q., Li, T.T., Lin, B.R., Lin, H.L., Liu, H., Liu, Q.Y., Liu, X.B., Liu, Y.F., Liu, Z., Liu, Z.D., Liu, Z., Lou, S.H., Lu, C.X., Luo, Y., Ma, W., McGushin, A., Niu, Y.L., Ren, C., Ren, Z.H., Ruan, Z.L., Schopp, W., Su, J., Tu, Y., Wang, J., Wang, Q., Wang, Y.Q., Wang, Y., Watts, N., Xiao, C.X., Xie, Y., Xiong, H., Xu, M.F., Xu, B., Xu, L., Yang, J., Yang, L.P., Yu, L., Yue, Y.J., Zhang, S.H., Zhang, Z.C., Zhao, J.Y., Zhao, L., Zhao, M.Z., Zhao, Z., Zhou, J.B., Gong, P., 2021. The 2020 China report of the Lancet Countdown on health and climate change. Lancet Public Health 6, E64–E81.

O, CARDONA, 1990. Terminología de Uso Común en Manejo de Riesgos. AGID, Report N 13. *EAFIT. Medellín*.

Cardona, O.D., van Aalst, M.K., Birkmann, J., Fordham, M., McGregor, G., Perez, R., Pulwarty, R.S., Schipper, E.L.F., Sinh, B.T., Decamps, H., Keim, M., Davis, I., Ebi, K.L., Lavell, A., Mechler, R., Murray, V., Pelling, M., Pohl, J., Smith, A.O., Thomalla, F., 2012. Determinants of risk: exposure and vulnerability. Managing the Risks of Extreme Events and Disasters to Advance Climate Change Adaptation 65–108.

Chen, X., Li, N., Liu, J.W., Zhang, Z.T., Liu, Y., Huang, C.F., 2020. Changes in global and regional characteristics of heat stress waves in the 21st Century. Earths Future 8, 17.

Chen, Y., Li, Y.i., 2017. An Inter-comparison of three heat wave types in china during 1961–2010: observed basic features and linear trends. Sci. Rep. 7 (1).

Ciais, P., Reichstein, M., Viovy, N., Granier, A., Ogee, J., Allard, V., Aubinet, M., Buchmann, N., Bernhofer, C., Carrara, A., Chevallier, F., de Noblet, N., Friend, A.D., Friedlingstein, P., Grunwald, T., Heinesch, B., Keronen, P., Knohl, A., Krinner, G., Loustau, D., Manca, G., Matteucci, G., Miglietta, F., Ourcival, J.M., Papale, D., Pilegaard, K., Rambal, S., Seufert, G., Soussana, J.F., Sanz, M.J., Schulze, E.D., Vesala, T., Valentini, R., 2005. Europe-wide reduction in primary productivity caused by the heat and drought in 2003. Nature 437, 529–533.

Dong, J.Q., Peng, J., He, X.R., Corcoran, J., Qiu, S.J., Wang, X.Y., 2020. Heatwave-induced human health risk assessment in megacities based on heat stress-social vulnerability-human exposure framework. Landscape Urban Plann. 203.

Dong, Z.Z., Wang, L., Sun, Y., Hu, T., Limsakul, A., Singhruck, P., Pimonsree, S., 2021. Heatwaves in southeast asia and their changes in a warmer world. *earths*. Future 9.

Dosio, A., Mentaschi, L., Fischer, E.M., Wyser, K., 2018. Extreme heat waves under 1.5 degrees C and 2 degrees C global warming. Environ. Res. Lett. 13.

Dubey, A.K., Lal, P., Kumar, P., Kumar, A., Dvornikov, A.Y., 2021. Present and future projections of heatwave hazard-risk over India: a regional earth system model assessment. Environ. Res. 201, 111573.

Feng, Y., Sun, F., Liu, W., Chen, J., Wang, H., Guo, Q., Wang, Y., Zhang, Q., Sang, Y.-F., 2022. Changes in compound hot and dry day and population exposure across China under climate change. Int. J. Climatol. 42 (5), 2935–2949.

Founda, D., Katavoutas, G., Pierros, F., Mihalopoulos, N., 2020. Centennial changes in heat waves characteristics in Athens (Greece) from multiple definitions based on climatic and bioclimatic indices. Global Planet. Change 212.

Gao, J.H., Sun, Y.Z., Liu, Q.Y., Zhou, M.G., Lu, Y.G., Li, L.P., 2015. Impact of extreme high temperature on mortality and regional level definition of heat wave: a multi-city study in China. Sci. Total Environ. 505, 535–544.

Garcia-Leon, D., Casanueva, A., Standardi, G., Burgstall, A., Flouris, A.D., Nybo, L., 2021. Current and projected regional economic impacts of heatwaves in Europe. Nat. Commun. 12, 10.

Harris, I., Jones, P.D., Osborn, T.J., Lister, D.H., 2014. Updated high-resolution grids of monthly climatic observations - the CRU TS3.10 Dataset. Int. J. Climatol. 34, 623–642.

HERSBACH, H., BELL, B., BERRISFORD, P., HIRAHARA, S., HORáNYI, A., MUñOZ-SABATER, J., NICOLAS, J., PEUBEY, C., RADU, R., SCHEPERS, D., SIMMONS, A., SOCI, C., ABDALLA, S., ABELLAN, X., BALSAMO, G., BECHTOLD, P., BIAVATI, G., BIDLOT, J., BONAVITA, M., DE CHIARA, G., DAHLGREN, P., DEE, D., DIAMANTAKIS, M., DRAGANI, R., FLEMMING, J., FORBES, R., FUENTES, M., GEER, A., HAIMBERGER, L., HEALY, S., HOGAN, R. J., HóLM, E., JANISKOVá, M., KEELEY, S., LALOYAUX, P., LOPEZ, P., LUPU, C., RADNOTI, G., DE ROSNAY, P., ROZUM, I., VAMBORG, F., VILLAUME, S. & THéPAUT, J.-N. 2020. The ERA5 global reanalysis. *Quarterly Journal of the Royal Meteorological Society,* 146, 1999-2049.

P. R, HOUSER, 2003. *The Global Land Data Assimilation System*, Data Assimilation for the Earth System.

Huang, W., Kan, H.D., Kovats, S., 2010. The impact of the 2003 heat wave on mortality in Shanghai, China. Sci. Total Environ. 408, 2418–2420.

L, JOHNSON, 2021. Alberta saw spike in reported deaths during heatwave, causes still under investigation.

Jones, B., O'Neill, B.C., 2016. Spatially explicit global population scenarios consistent with the Shared Socioeconomic Pathways. Environ. Res. Lett. 11.

Kazmierczak, A., Cavan, G., 2011. Surface water flooding risk to urban communities: Analysis of vulnerability, hazard and exposure. Landscape Urban Plann. 103, 185–197.

Kobayashi, S., Ota, Y., Harada, Y., Ebita, A., Moriya, M., Onoda, H., Onogi, K., Kamahori, H., Kobayashi, C., Endo, H., Miyaoka, K., Takahashi, K., 2015. The JRA-55 Reanalysis: General Specifications and Basic Characteristics. J. Meteorol. Soc. Jpn 93, 5–48.

Lehner, F., Stocker, T.F., 2015. From local perception to global perspective. Nat. Clim. Change 5, 731–734.

Liu, Y., Zhang, Z., Chen, X., Huang, C., Han, F., Li, N., 2021. Assessment of the Regional and Sectoral Economic Impacts of Heat-Related Changes in Labor Productivity Under Climate Change in China. *Earth's*. Future 9.

V, MASSON-DELMOTTE, P, ZHAI, A, PIRANI, S. L, CONNORS, C, PéAN, S, BERGER, N, CAUD, Y, CHEN, L, GOLDFARB, M. I, GOMIS, M, HUANG, K, LEITZELL, E, LONNOY, J. B. R, MATTHEWS, T. K, MAYCOCK, T, WATERFIELD, O, YELEKçI, R, YU, B, ZHOU, 2021. IPCC, 2021: Climate Change 2021: The Physical Science Basis. Contribution of Working Group I to the Sixth Assessment Report of the Intergovernmental Panel on Climate Change.

Meehl, G.A., Tebaldi, C., 2004. More intense, more frequent, and longer lasting heat waves in the 21st century. Science 305, 994–997.

Mitchell, D., Kornhuber, K., Huntingford, C., Uhe, P., 2019. The day the 2003 european heatwave record was broken Comment. Lancet Planetary Health 3, E290–E292.

Moss, R.H., Edmonds, J.A., Hibbard, K.A., Manning, M.R., Rose, S.K., van Vuuren, D.P., Carter, T.R., Emori, S., Kainuma, M., Kram, T., Meehl, G.A., Mitchell, J.F.B., Nakicenovic, N., Riahi, K., Smith, S.J., Stouffer, R.J., Thomson, A.M., Weyant, J.P., Wilbanks, T.J., 2010. The next generation of scenarios for climate change research and assessment. Nature 463, 747–756.

Murakami, D., Yoshida, T., Yamagata, Y., 2021. Gridded GDP projections compatible with the Five SSPs (Shared Socioeconomic Pathways). *Frontiers*. Built Environment 7.

Panda, D.K., Aghakouchak, A., Ambast, S.K., 2017. Increasing heat waves and warm spells in India, observed from a multiaspect framework. J. Geophys. Res.-Atmospheres 122, 3837–3858.

Parente, J., Pereira, M.G., Amraoui, M., Fischer, E.M., 2018. Heat waves in Portugal: current regime, changes in future climate and impacts on extreme wildfires. Sci. Total Environ. 631–632, 534–549.

Perkins-Kirkpatrick, S.E., Lewis, S.C., 2020. Increasing trends in regional heatwaves. *Nature*. Communications 11.

S. E, PERKINS, 2015. A review on the scientific understanding of heatwaves-Their measurement, driving mechanisms, and changes at the global scale. *Atmospheric Research,* 164, 242-267.

Perkins, S.E., Alexander, L.V., 2013. On the Measurement of Heat Waves. J. Clim. 26, 4500–4517.

Perkins, S.E., Alexander, L.V., Nairn, J.R., 2012. Increasing frequency, intensity and duration of observed global heatwaves and warm spells. Geophys. Res. Lett. 39.

POTESTIO, M. L. J. I. R. 2021. Estimate on number of suspected heat-related deaths rises to 808.

Raei, E., Nikoo, M.R., Aghakouchak, A., Mazdiyasni, O., Sadegh, M., 2018. Data Descriptor: GHWR, a multi-method global heatwave and warm-spell record and toolbox. Sci. Data 5.

Rodell, M., Houser, P.R., Jambor, U., Gottschalck, J., Mitchell, K., Meng, C.-J., Arsenault, K., Cosgrove, B., Radakovich, J., Bosilovich, M., Entin, J.K., Walker, J.P., Lohmann, D., Toll, D., 2004. The global land data assimilation system. Bull. Am. Meteorol. Soc. 85 (3), 381–394.

Roye, D., Codesido, R., Tobias, A., Taracido, M., 2020. Heat wave intensity and daily mortality in four of the largest cities of Spain. Environ. Res. 182.

Schumacher, D.L., Keune, J., van Heerwaarden, C.C., Vilà-Guerau de Arellano, J., Teuling, A.J., Miralles, D.G., 2019. Amplification of mega-heatwaves through heat torrents fuelled by upwind drought. Nat. Geosci. 12 (9), 712–717.

Stefanon, M., D'Andrea, F., Drobinski, P., 2012. Heatwave classification over Europe and the Mediterranean region. Environ. Res. Lett. 7.

Stott, P.A., Stone, D.A., Allen, M.R., 2004. Human contribution to the European heatwave of 2003. Nature 432, 610–614.

Sun, Y., Hu, T., Zhang, X.B., 2018. Substantial Increase in Heat Wave Risks in China in a Future Warmer World. Earths Future 6, 1528–1538.

Tuholske, C., Caylor, K., Funk, C., Verdin, A., Sweeney, S., Grace, K., Peterson, P., Evans, T., 2021. Global urban population exposure to extreme heat. PNAS 118, 9.

UGUEN-CSENGE, E. 2021. For 3rd straight day, B.C. village smashes record for highest Canadian temperature at 49.6 C.

Ullah, I., Saleem, F., Iyakaremye, V., Yin, J., Ma, X.Y., Syed, S., Hina, S., Asfaw, T.G., Omer, A., 2022. Projected Changes in Socioeconomic Exposure to Heatwaves in South Asia Under Changing Climate. Earths Future 10, 19.

van der Velde, M., Wriedt, G., Bouraoui, F., 2010. Estimating irrigation use and effects on maize yield during the 2003 heatwave in France. Agric. Ecosyst. Environ. 135, 90–97.

Vautard, R., Gobiet, A., Jacob, D., Belda, M., Colette, A., Deque, M., Fernandez, J., Garcia-Diez, M., Goergen, K., Guttler, I., Halenka, T., Karacostas, T., Katragkou, E., Keuler, K., Kotlarski, S., Mayer, S., van Meijgaard, E., Nikulin, G., Patarcic, M., Scinocca, J., Sobolowski, S., Suklitsch, M., Teichmann, C., Warrach-Sagi, K., Wulfmeyer, V., Yiou, P., 2013. The simulation of European heat waves from an ensemble of regional climate models within the EURO-CORDEX project. Clim. Dyn. 41, 2555–2575.

Vittal, H., Karmakar, S., Ghosh, S., Murtugudde, R., 2020. A comprehensive India-wide social vulnerability analysis: highlighting its influence on hydro-climatic risk. Environ. Res. Lett. 15.

Wang, J., Chen, Y., Liao, W., He, G., Tett, S.F.B., Yan, Z., Zhai, P., Feng, J., Ma, W., Huang, C., Hu, Y., 2021. Anthropogenic emissions and urbanization increase risk of compound hot extremes in cities. *Nature*. Clim. Change 11 (12), 1084–1089.

Wang, J., Feng, J.M., Yan, Z.W., Chen, Y., 2020. Future risks of unprecedented compound heat waves over three vast urban agglomerations in china. *earths*. Future 8.

Wang, Y., Nordio, F., Nairn, J., Zanobetti, A., Schwartz, J.D., 2018. Accounting for adaptation and intensity in projecting heat wave-related mortality. Environ. Res. 161, 464–471.

Weng, Y.-W., Cai, W.-J., Wang, C., 2020. The application and future directions of the Shared Socioeconomic Pathways (SSPs). Climate Change Research 16, 215–222.

Williams, S., Nitschke, M., Weinstein, P., Pisaniello, D.L., Parton, K.A., Bi, P., 2012. The impact of summer temperatures and heatwaves on mortality and morbidity in Perth, Australia 1994–2008. Environ. Int. 40, 33–38.

Wondmagegn, B.Y., Xiang, J., Dear, K., Williams, S., Hansen, A., Pisaniello, D., Nitschke, M., Nairn, J., Scalley, B., Varghese, B.M., Xiao, A., Jian, L.e., Tong, M., Bambrick, H., Karnon, J., Bi, P., 2021. Impact of heatwave intensity using excess heat factor on emergency department presentations and related healthcare costs in Adelaide, South Australia. Sci. Total Environ. 781, 146815.

Xu, C., Kohler, T.A., Lenton, T.M., Svenning, J.C., Scheffer, M., 2020. Future of the human climate niche. PNAS 117, 11350–11355.

Y, YAMAGATA, D, MURAKAMI, T, YOSHIDA, 2019. Spatiotemporal Heatwave Risk Evaluation: Considering Hazard, Exposure, and Vulnerability. *2019 Ieee International Geoscience and Remote Sensing Symposium (Igarss 2019)*, 5524-5527.

Yang, J., Yin, P., Sun, J.M., Wang, B.G., Zhou, M.G., Li, M.M., Tong, S.L., Meng, B.H., Guo, Y.M., Liu, Q.Y., 2019. Heatwave and mortality in 31 major Chinese cities: definition, vulnerability and implications. Sci. Total Environ. 649, 695–702.

C, YIN, F, YANG, J. L, WANG, Y. X, YE, 2020, Spatiotemporal Distribution and Risk Assessment of Heat Waves Based on Apparent Temperature in the One Belt and One Road Region. *Remote Sensing,* 12.

Yin, Q., Wang, J.F., Ren, Z.P., Li, J., Guo, Y.M., 2019. Mapping the increased minimum mortality temperatures in the context of global climate change. *Nature*. Communications 10.

S, YU, S. F. B, TETT, N, FREYCHET, Z. W, YAN, 2021, Changes in regional wet heatwave in Eurasia during summer (1979-2017). *Environmental Research Letters,* 16.

Zhao, M., Lee, J.K.W., Kjellstrom, T., Cai, W., 2021. Assessment of the economic impact of heat-related labor productivity loss: a systematic review. Clim. Change 167 (1-2).

Zittis, G., Hadjinicolaou, P., Almazroui, M., Bucchignani, E., Driouech, F., el Rhaz, K., Kurnaz, L., Nikulin, G., Ntoumos, A., Ozturk, T., Proestos, Y., Stenchikov, G., Zaaboul, R., Lelieveld, J., 2021. Business-as-usual will lead to super and ultra-extreme heatwaves in the Middle East and North Africa. npj Clim. Atmos. Sci. 4, 9.